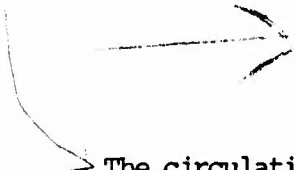


LIFTING SURFACE THEORY FOR THRUST AUGMENTING EJECTORS

by

Dr. P. M. Bevilacqua
Rockwell International
Columbus, Ohio



The circulation theory of airfoil lift has been applied to predict the static performance of thrust augmenting ejectors. The ejector shroud is considered to be "flying" in the velocity field induced by the entrainment of the primary jets, so that the thrust augmenting force is viewed as analogous to the lift on a wing. Vortex lattice methods are used to compute the augmentation from the surface pressures on the shroud. The thrust augmentation is shown to depend on the length and shape of the shroud, as well as its position and orientation. Predictions of this new theory are compared with the results of classical momentum theories for calculating the augmentation from the stream thrust.



Copyright AIAA. Reprinted with Permission.

INTRODUCTION

For their whole lives, scientists are said to have a special respect for the man who started them off. It's true; and that will always be my feeling for Dr. Hans von Ohain. My first job after college was to develop some of his ideas on ejector thrust augmentation. This experience influenced the direction of my career: his enthusiasm for the subject was contagious, and I have never lost interest in ejectors. He also influenced the theme of the paper I have selected for this volume: the existence of mechanical analogies to the augmentation process, such as the one described in the first part of this paper, was suggested by Hans.* This analogy led me to the circulation model which is the subject of the paper.

An ejector is a pneumatic device that uses entrainment by a jet of primary fluid to pump a secondary flow. Significant increases in the static thrust of turbojet engines can be obtained by diverting the exhaust jet through an ejector pump. In this application, the ejector functions like a ducted fan. Thrust is increased by accelerating a large mass of air drawn from the atmosphere. Since ejectors can be used to deflect as well as augment the engine thrust, the additional lift necessary to give an aircraft V/STOL capabilities can be developed from an engine sized for efficient cruise. When the ejector is integrated with the wing to produce a lift-propulsion system, the exhaust flow acts like a jet flap to increase the circulation lift of the wing, and thus provide good STOL performance. In addition, separate reaction jets are not required for control during hover. In order to demonstrate this technology, Rockwell International presently is constructing the XFV-12A, a Navy V/STOL aircraft employing ejectors in the wing and canard (Figure 1.).

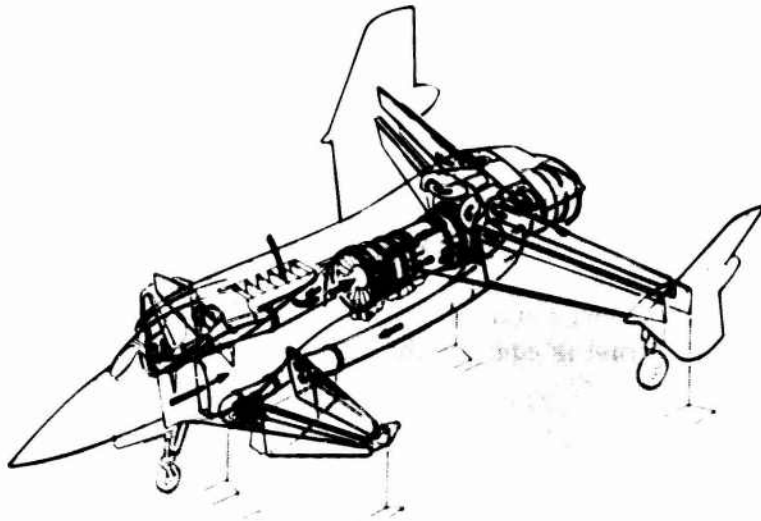


Figure 1. XFV-12A Ejector Technology Demonstrator Aircraft

*A similar analogy has been developed by our colleague, H. Viets⁵.

Analytic procedures for calculating ejector performance are necessary to guide research and for preliminary design studies. The analytic methods that have been developed to date are based broadly on von Kármán's now classical momentum analysis.¹ These methods²⁻⁴ deal only with the flow inside the ejector. The thin shear layer approximations are applied to reduce the governing elliptic equations to a parabolic set, which can be solved by marching through the ejector in the streamwise direction. This approach has been useful in identifying some of the factors that affect the level of augmentation and in predicting the results of particular changes in the ejector geometry. However, since elliptic effects are neglected, these solutions are limited to cases in which the ejector is relatively long and the diffuser angle is small.

The purpose of this paper is to demonstrate that elliptic effects can be included in the analysis of ejector performance by a relatively straightforward extension of vortex lattice methods. The ejector shroud is replaced by a distribution of bound vortices, and the primary jet is represented by a line of sinks on the ejector axis. However, the thickness of the jet is neglected, so that only performance trends are predicted. In the following section, the principle of thrust augmentation will be described. The hypothesis that a circulation is generated around the ejector shroud is used in the next section for the development of a new ejector model. In the final section, the predictions of this new model are compared with classical solutions, and the method is then used to examine the effect of changing the position and shape of the shroud.

PRINCIPLE OF THRUST AUGMENTATION

Nonconservative Collisions

All fluid propulsion devices develop thrust by imparting momentum to a fluid stream. By Newton's law of action and reaction, the propulsor experiences a force that is equal and opposite to the momentum change of the fluid, $T = \dot{m}v$. A turbojet engine draws air from the atmosphere and adds energy in the form of heat by the combustion of some fuel. The thermal energy of the hot gas is converted to the kinetic energy of an exhaust jet by accelerating the gas through a nozzle. The engine thrust is equal to the momentum change of the air drawn through it.

A thrust-augmenting ejector also adds energy to air drawn from the atmosphere, but by the direct transfer of kinetic energy from the primary jet. The mechanism of energy transfer is the turbulent mixing of the two streams. Since the mixing process is basically a collision between the jet and the surrounding fluid, the

mechanism by which the thrust is increased may be understood through the consideration of a collision between two generalized masses. Assume that a particle of mass m_1 impacts and remains embedded in a stationary mass m_2 . Such a collision is said to be completely inelastic. In the absence of external forces, momentum is conserved, and the particles move off together at a speed u_{12} such that

$$m_1 u_1 = (m_1 + m_2) u_{12} \quad (1)$$

The initial kinetic energy of the first mass is $\frac{1}{2} m_1 u_1^2$, and the kinetic energy of the two-mass system after the collision is $\frac{1}{2} (m_1 + m_2) u_{12}^2$. Their ratio is the energy transfer efficiency.

$$\eta = \frac{\frac{1}{2} (m_1 + m_2) u_{12}^2}{\frac{1}{2} m_1 u_1^2} = \frac{m_1}{m_1 + m_2} \quad (2)$$

so that a fraction of the initial kinetic energy is lost to heat and other forms of random energy during the impact. The quantity of energy lost does not depend on the mechanics of the collision or the substance of which the particles are composed, but only on the ratio of their masses, as given by Eq. (2). Thus, there is no augmentation in this case, and a fraction of the kinetic energy, which depends only on the ratio of the masses, is dissipated in the collision.

However, if both particles are accelerated by an external force before the impact, the momentum is increased. Suppose, for example, that both particles are negatively charged and that the impact occurs after they have been accelerated by the attraction along the axis of a positively charged ring, as shown in Figure 2. At a distance d far from the ring, the momentum of the first mass is $m_1 u_1$, and

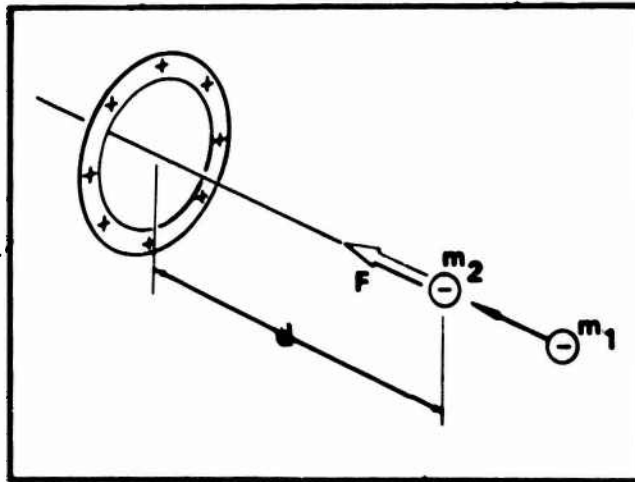


Figure 2. Attraction by the Charged Ring Produces an Augmentation of the Particle Momentum

the second mass is at rest. At the center of the ring, just before the impact, the velocities are

$$u_1^* = (u_1^2 + 2ad)^{\frac{1}{2}} \quad (3)$$

$$u_2^* = (2ad)^{\frac{1}{2}} \quad (4)$$

in which a is the average acceleration over the distance d . Momentum is conserved during the impact itself. If the two masses do not separate after the collision but become embedded or stick together, the conservation of momentum requires that

$$m_1 u_1^* + m_2 u_2^* = (m_1 + m_2) u_{12}^* \quad (5)$$

The embedded masses decelerate together behind the ring. By reason of symmetry, the average decelerating force is equal and opposite to the force of attraction. The final velocity of the embedded masses is therefore

$$u_{12} = (u_{12}^* - 2ad)^{\frac{1}{2}} \quad (6)$$

The ratio of the momentum after the collision $(m_1 + m_2) u_{12}^*$ to the initial momentum $m_1 u_1$ may be evaluated by substituting in turn for u_{12} then u_{12}^* and finally for u_1^* and u_2^* . Performing these substitutions yields, for this ratio,

$$\beta = \sqrt{1 + 2M [(H^2 + H)^{\frac{1}{2}} - H]} \quad (7)$$

in which M is the ratio of the masses, $M = m_2/m_1$, and H is the ratio of the potential energy of the charge separation to the initial kinetic energy,

$$H = ad/\frac{1}{2}u_1^2 \quad (8)$$

The energy transfer efficiency can be evaluated by making the same substitutions for u_{12} . The result is

$$\eta = \beta^2/(1 + M) \quad (9)$$

If the charge on the ring is relatively small, then $H \ll 1$, and the collision reduces to the case of one mass striking another in the absence of an accelerating potential. There is no momentum increase, $\beta=1$, and only a fraction of the initial kinetic energy is transferred, $\eta=1/(1+M)$, the remainder being dissipated during the collision. Thus, in the absence of external forces, momentum is conserved, and some kinetic energy is lost. On the other hand, if the charge on the ring is large,

then $H \gg 1$, and the momentum ratio simplifies to

$$\phi = (1 + M)^{\frac{1}{2}} \quad (10)$$

so that the momentum increases and all of the initial kinetic energy is transferred, $\eta = 1$. For example, if m_2 has three times the mass of m_1 , the initial momentum is doubled. The dependence of ϕ and η on intermediate values of H is sketched in Figures 3 and 4. Thus, when the collision occurs in this kind of potential energy well, the transfer of kinetic energy and the final momentum both increase.

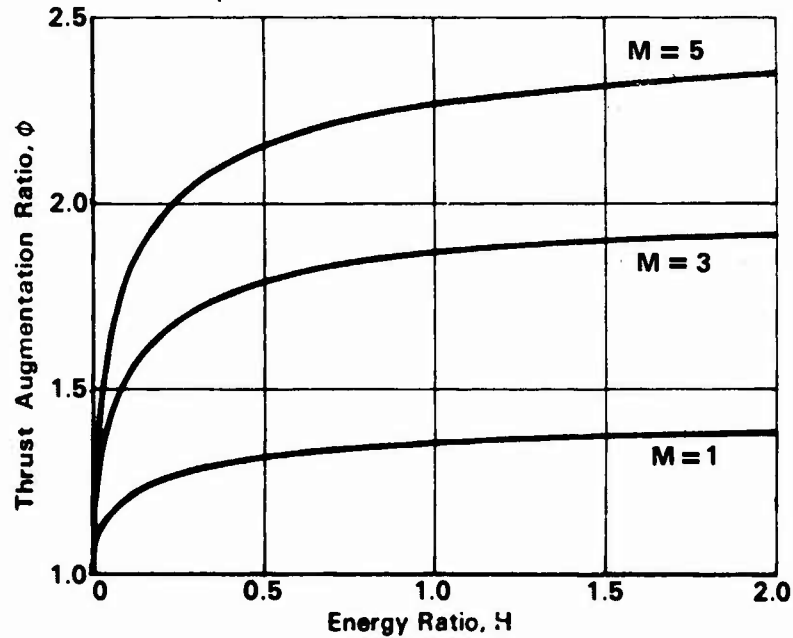


Figure 3. The Augmentation Ratio Increases with the Initial Mass and Energy Ratios

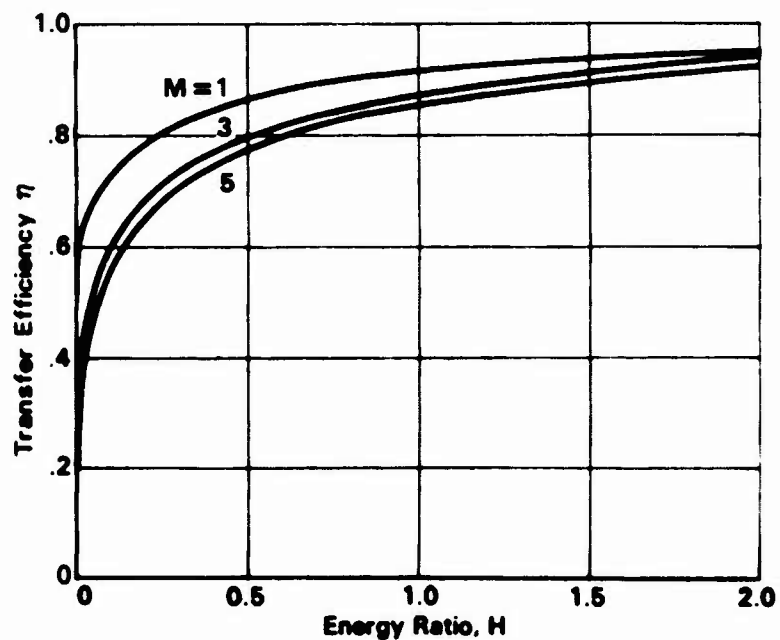


Figure 4. The Transfer of Kinetic Energy Increases with the Initial Potential Energy

The fundamental reason that momentum increases is that the transfer of kinetic energy increases. If both masses are accelerated through the same potential before impact, the absolute velocity difference between them is reduced; that is,

$$u_1^* - u_2^* \leq u_1 \quad (11)$$

and the force of the impact consequently diminishes. In the limit of an infinitely deep well, the velocity difference goes to zero, and there is no impact. Therefore, if the masses stick together, all of the initial kinetic energy is transferred, and the momentum increases accordingly. Another view of the same process is that the total time during which both masses are being accelerated is longer than the time during which they are being decelerated, because $u_{12} > 0$. Thus, over the duration of the interaction, the masses experience a net acceleration from the charged ring. This is the origin of the momentum increase.

Jet Thrust Augmentation

The jet mixing process is basically an inelastic collision between the jet and the surrounding fluid. As such, jet mixing is governed by the same laws of momentum and energy conservation as simple collisions between discrete particles. In free jet mixing, the momentum flux is conserved, and there is a corresponding loss of kinetic energy which is transformed to turbulence and heat. However, suppose that the jet passes through a region in which the static pressure is ΔP less than atmospheric pressure, as sketched in Figure 5. Both the jet and the

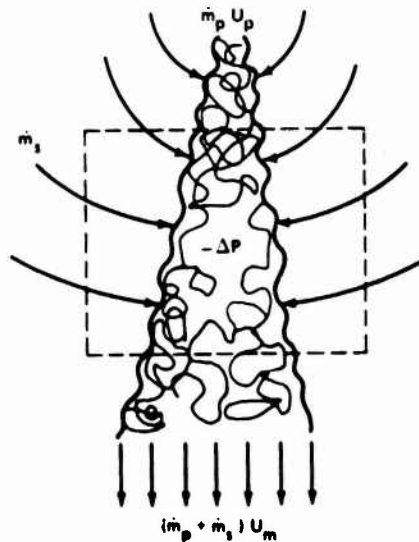


Figure 5. Jet Mixing in a Region of Reduced Pressure Increases the Initial Jet Thrust

fluid that mixes with it must accelerate upon entering the low-pressure region. Inside the region, before mixing, the flow velocities are given approximately by Bernoulli's equation,

$$U_p^* = \left[U_p^2 + (2 \Delta P / \rho) \right]^{1/2} \quad (12)$$

$$U_s^* = (2 \Delta P / \rho)^{1/2} \quad (13)$$

in the primary and secondary streams, respectively. Momentum is conserved during the mixing process itself, so that

$$\dot{m}_p U_p^* + \dot{m}_s U_s^* = (\dot{m}_p + \dot{m}_s) U_m^* \quad (14)$$

The mixed stream decelerates as it leaves the low-pressure region, and its final velocity is

$$U_m = \left[U_m^{*2} - (2 \Delta P / \rho) \right]^{1/2} \quad (15)$$

By comparing these relations with those for the collision between discrete particles, it can be seen that the low-pressure region has the same role as the potential well. The velocity difference between the mixing streams is reduced in the low-pressure region, and so the transfer of kinetic energy increases. The corresponding increase in momentum flux has the same dependence on M and H as in the simple collision; that is

$$\phi = \sqrt{1 + 2M \left[(H^2 + H)^{1/2} - H \right]} \quad (16)$$

except that M is defined in terms of the mass flux ratio, $M = \dot{m}_s / \dot{m}_p$, and H is the ratio of the static pressure drop to the initial kinetic energy, $H = \Delta P / \frac{1}{2} \rho U_p^2$.

If the pressure drop is negligibly small, $H \ll 1$, and the solution reduces to the case of free jet mixing. Momentum is conserved, $\phi = 1$. On the other hand, if the pressure drop is relatively large, $H \gg 1$, and the momentum ratio reduces to

$$\phi = (1 + M)^{1/2} \quad (17)$$

so that the thrust increases with the entrainment ratio.

Of course, low-pressure regions do not just occur; however, one can be produced by simply passing a portion of the jet through a shroud, as shown in Figure 6. The entrained flow must accelerate as it enters the shroud, and, according to Bernoulli's equation, the pressure will drop accordingly. The pumping action of the jet thus establishes its own low-pressure region within the ejector shroud. In this case, the pressure drop H is a function of the entrainment M . When the mixed stream returns to ambient pressure behind the shroud, it has greater thrust than the original jet. The ratio of the final thrust to the initial thrust is the augmentation ratio, and the shroud acts as a thrust-augmenting ejector.

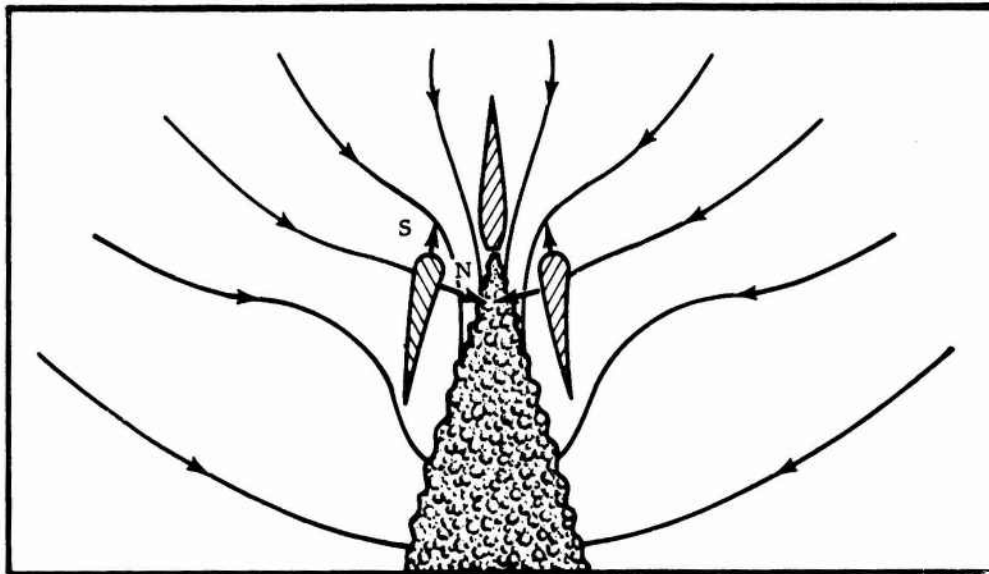


Figure 6. The Ejector Shroud Develops a Force Analogous to the Lift on a Wing

LIFTING SURFACE HYPOTHESIS

Circulation and Elliptic Effects

Except for the simple case of the long, straight shroud analyzed by von Kármán,¹ a unique solution for H in terms of M does not exist. This is because the Navier-Stokes equations for steady fluid motion are elliptic, which means that the domain of influence of a point disturbance is the entire flow volume; that is, pressure and stress gradients transmit the effect of local disturbances to every other point in the flow. Thus, the flow through the ejector, given by the values of M and H , depends on boundary conditions outside the ejector as well as inside the shroud.

In order to calculate the thrust augmentation without solving the full Navier-Stokes equations for the entire flowfield, some approximations must be made. The classical approach is based on streamwise integration of the momentum and continuity equations. If the ejector is relatively long and the diffuser angle is small, the primary direction of flow is through the ejector, so that gradients of the normal stresses and the variation of pressure across the flow can be neglected within the ejector. This thin shear layer approximation reduces the governing elliptic equations to a parabolic set. In parabolic flows, the effect of a disturbance is confined to regions downstream of the disturbance, so that the equations can be solved by marching through the ejector in the streamwise direction. The solution is obtained by iterating on the inlet velocity until the exhaust pressure matches the atmospheric pressure outside the ejector. This approach is equivalent to determining H and M as functions of the jet mixing rate and the shape of the duct.

Although the elliptic boundary value problem can thus be transformed to an initial value problem that is more easily solved, the fundamental elliptic character of the flowfield is unchanged. This means that there are configurations for which the classical thin shear layer approximation predicts the wrong performance or does not yield a solution at all. For instance, as the walls of the shroud are removed to infinity, the predicted thrust augmentation ratio does not reduce to unity,^{1,3} as it must in the limit of an isolated turbulent jet. Also, when the ejector is short or the diffuser angle is large, the exhaust pressure is less than atmospheric pressure. This pressure difference is supported by the momentum of the exhaust jet, whereas the jet momentum depends, in turn, on the pressure difference. Thus, the exhaust pressure becomes a floating boundary condition, and a unique solution to the initial value problem does not exist.

In the following sections, the circulation theory of aerodynamic lift is utilized to predict the primary elliptic effects on ejector performance. The pressure and velocity of the secondary flow drawn through the ejector are controlled by the shroud. An isolated jet induces an essentially lateral flow, as seen in Figure 5. However, this induced flow is redirected through the ejector by a circulation generated around each of the shroud sections. The lifting surface hypothesis is that the shroud "flies" in the velocity field of the fluid entrained by the jet and experiences a force related to the lift developed on a wing fixed in a moving stream. The thrust augmentation is the ratio of the primary jet thrust T plus the axial force on the flaps F to the isentropic thrust of the primary mass,

$$\theta = (T + F) / \dot{m}V \quad (18)$$

The external velocity field is calculated by superpositioning a distribution of bound vortex elements, which represent the shroud, and a stream function for the flow induced by the jet. The vorticity distribution is determined by solving a system of equations which specifies that the vortex sheet must be a streamline. The force on the duct is then computed as the cross product of the bound vorticity and the velocity induced by the jet. By using vortex lattice methods for this calculation, the Kutta condition is automatically satisfied. This, in turn, sets the ejector inlet and exhaust pressures, which is the primary elliptic effect.

Entrainment Function

The stream function that describes the secondary flow induced by the isolated primary jet must be harmonic and satisfy the entrainment boundary condition on the surface of the jet. In a self-preserving turbulent jet, all velocities decay as $x^{-1/2}$, and so the entrainment velocity U_e was assumed to vary as

$$U_e = U_0 (x/t)^{-1/2} \quad (19)$$

in which t is the nozzle gap and U_0 is a free constant that depends on the entrainment rate of the jet.

Although a solution for the velocity field can be obtained numerically, by locating a line of sinks on the surface of the jet and then adding the induced velocities at each point, an analytic solution is easy to obtain. The form of the boundary condition suggests a solution in polar coordinates. Let us define a stream function $\psi(r, \theta)$ such that $U_r = -r^{-1}(\partial\psi/\partial\theta)$ and $U_\theta = \partial\psi/\partial r$. Any function of the form

$$\psi = r^k (A \sin k\theta + B \cos k\theta) \quad (20)$$

is harmonic. If it is assumed that the origin of coordinates is at the nozzle exit and the spreading angle of the jet is small, the boundary conditions on ψ become

$$\left. \frac{\partial\psi}{\partial r} \right|_{\theta=0} = -U_0 \left(\frac{x}{t} \right)^{-1/2} \quad (21)$$

$$\left. \frac{\partial\psi}{\partial r} \right|_{\theta=\pi} = 0 \quad (22)$$

so that the stream function for the potential flow external to the jet is

$$\psi = -2U_0(rt)^{1/2} \cos(\theta/2) \quad (23)$$

The boundary condition on the other side of the jet is satisfied automatically. The streamlines of this solution are sketched in Figure 7.

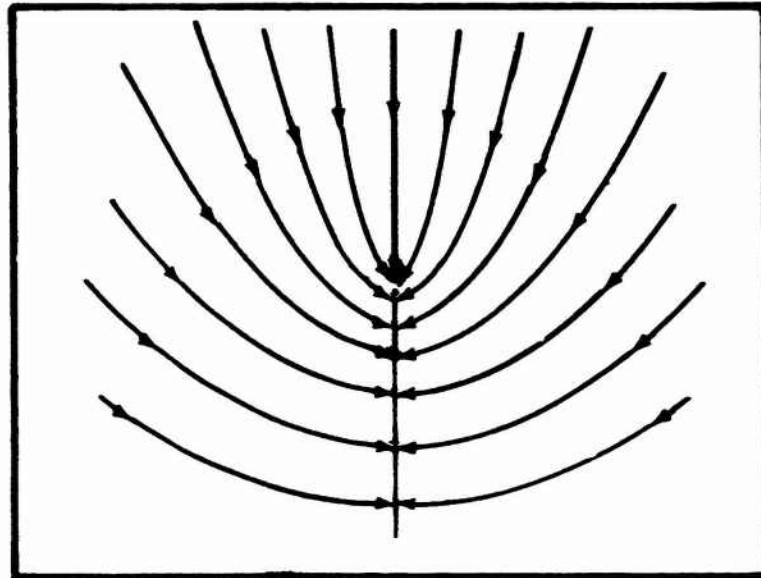


Figure 7. Streamlines of the Flow Entrained into an Isolated Jet

Vorticity Distribution

A conventional vortex lattice representation of the ejector shroud was utilized to determine the circulation generated around each section. The continuous vorticity distribution is replaced by n discrete vortices of strength γ_j located at x_j , the quarter-chord of the panels shown in Figure 8. In keeping with the

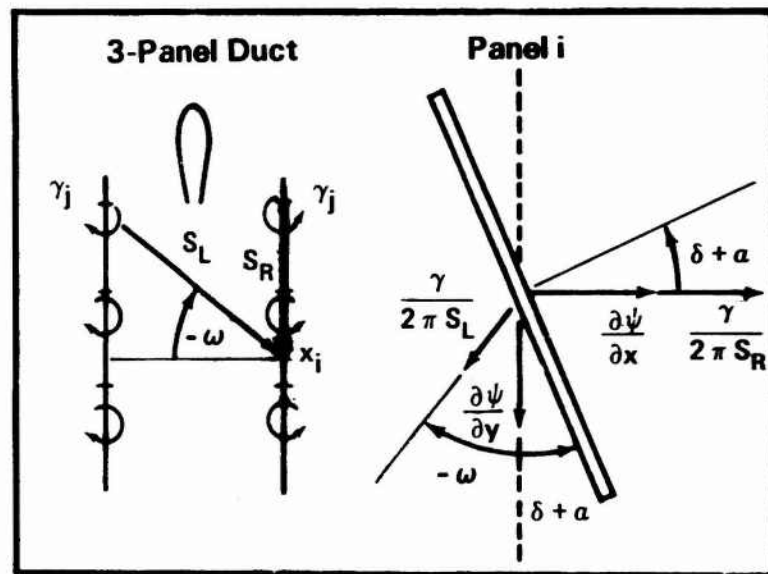


Figure 8. Vortex Panel Representation of the Ejector Shroud

assumption that the jet is thin, a planar wing approximation has been used to linearize the boundary-value problem. This approximation amounts to satisfying the boundary conditions on the chord line of the ejector shroud instead of on its surface. The appropriate boundary condition is that of zero flow through the shroud.

This boundary condition is satisfied at n control points corresponding to the three-quarter-chord station of the panels, that is, midway between the vortices. This is shown in Figure 8 also. The component of the jet-induced velocity normal to the i panel at the control point x_i is

$$U_i = \frac{\partial \psi}{\partial y} \sin(\delta + \alpha_i) + \frac{\partial \psi}{\partial x} \cos(\delta + \alpha_i) \quad (24)$$

in which δ is the mean diffuser angle determined by the chord line of the airfoil sections, and α is the angle of the i panel relative to the mean chord line. The case $\delta = \alpha_i = 0$ corresponds to a straight ejector duct.

In calculating the velocity induced by the vortex sheet, it is convenient to consider simultaneously the effect of each vortex and its image on the opposite side. The contribution to the velocity normal to the i panel by the vortex pair of strength γ_j is

$$W_i = \left[\frac{\cos(\delta + \alpha_i)}{2\pi S_{jL}} - \frac{\sin(\delta + \alpha_i - \omega_{ij})}{2\pi S_{jR}} \right] \gamma_j \quad (25)$$

The position vectors S_{jL} and S_{jR} are directed from the vortices to the control point on the panel, as shown in Figure 8. The angular position vector

$$\omega_{ij} = \tan^{-1} [(x_j - x_i)/(y_j + y_i)] \quad (26)$$

refers to the location of the image vortex on the opposite side. The total velocity induced at each panel is obtained by adding the contribution of all of the vortices from the leading edge to the trailing edge of the shroud.

The resultant of the normal velocities induced by the jet and the vortex sheet must be zero if the shroud is to be a streamline of the flow. Thus, on each panel, W_i is set equal but opposite to U_i :

$$-U_i = C_{ij} \gamma_j \quad (27)$$

The influence coefficients C_{ij} have the form given in Eq. (25). The summation convention for repeated indices is intended to apply. Thus, this expression represents a set of n simultaneous algebraic equations. This set was solved for the γ_j by triangularization of the matrix C_{ij} .

Axial Thrust

The thrust of the ejector is the sum of the initial jet thrust plus the axial thrust on the shroud. The basis of the present method is the assumption that the shroud thrust can be calculated from the normal force and leading-edge suction given for the airfoil by the vortex lattice method. These forces are shown in Figure 6. Because the inviscid leading-edge suction force is essentially independent of the leading-edge radius, the planar wing approximation does not place a restriction on the solution in this respect. However, since a contribution to the total force is determined for each panel, the vortex lattice method essentially redistributes the leading-edge suction over the entire chord. As discussed by Hancock⁶ and Kalman et al.,⁷ this is characteristic of the method. If a sufficient number of panels are used, the suction is concentrated near the leading edge, and satisfactory results are obtained.

The total force on each panel is determined by the interaction of the bound vortex and the velocity field induced by the jet and all of the other vortices. However, the axial component of the net thrust on the shroud is given by the cross product of the entrainment velocity component normal to the ejector axis and the vortex strength:

$$F_i = \rho \frac{\partial \psi_i}{\partial x_i} \gamma_i \quad (28)$$

The total thrust is obtained by summing the contribution of each of the panels, $F = \sum F_i$. Because the mutually induced forces on any two vortices are equal and opposite, the effect of the other vortices does not contribute to the net axial thrust and does not appear in Eq. (28). On the other hand, the mutually induced forces are important in determining the pressure distribution and absolute forces on each section of the shroud.

The jet thrust is calculated from the momentum flux at the origin of the jet,

$$T = \rho V_0^2 t \quad (29)$$

in which t is the nozzle gap and V_0 is the initial jet velocity. Since the static pressure in the throat of the ejector can fall several pounds per square inch

below atmospheric pressure, the nozzle thrust actually varies with the circulation. This produces a small but not insignificant contribution to the augmentation. The thrust augmentation ratio is therefore defined to be

$$\Phi = (T + \Sigma F_i)/T' \quad (30)$$

The reference thrust T' is the isentropic thrust obtained by expanding the same mass of primary fluid, $m = \rho V_0 t$, to atmospheric pressure. The reference jet thus has the same power requirements as the primary jet of the augmentser.

Because the presence of the shroud reduces the entrainment of the jet, it is necessary to iterate between the strength of the vortex sheet and the rate of jet entrainment. In the stream function for the induced velocities, the rate of entrainment is specified by the initial entrainment velocity U_0 . This velocity is related to the initial jet velocity V_0 according to the relation

$$U_0 = (2/R_T) (V_0 - U_s) \quad (31)$$

The turbulent Reynolds number R_T is an empirical constant that has a value of approximately 25 in turbulent jets,⁷ and U_s is the total induced velocity at the ejector inlet. The change in the entrainment was estimated by iterating between the circulation and the inlet velocity through Eq. (31). This approach is similar to that used in coupling a solution for the boundary-layer displacement thickness to a solution for the external flow.

RESULTS AND DISCUSSION

Primary Ejector Geometry

From classical ejector analysis,^{1,9} it is concluded that the thrust augmentation ratio increases with the ejector inlet and diffuser area ratios, and as the mixing of the primary and secondary streams becomes more complete. The effect of length is not explicitly calculated, but insofar as mixing increases with length, it is inferred that augmentation does also. With the lifting surface method described here, the effect of varying the ejector length can be calculated directly. In Figure 9, the predicted change in augmentation with inlet area ratio for three different duct lengths is shown. All dimensions are normalized with the nozzle gap t . It can be seen that, for constant inlet area ratio, the augmentation increases with the length of the shroud.

The effect of varying the shroud length in conjunction with the throat width can also be estimated. There are two important cases to consider. The first is that in which the length of the shroud is held constant while the inlet area ratio is

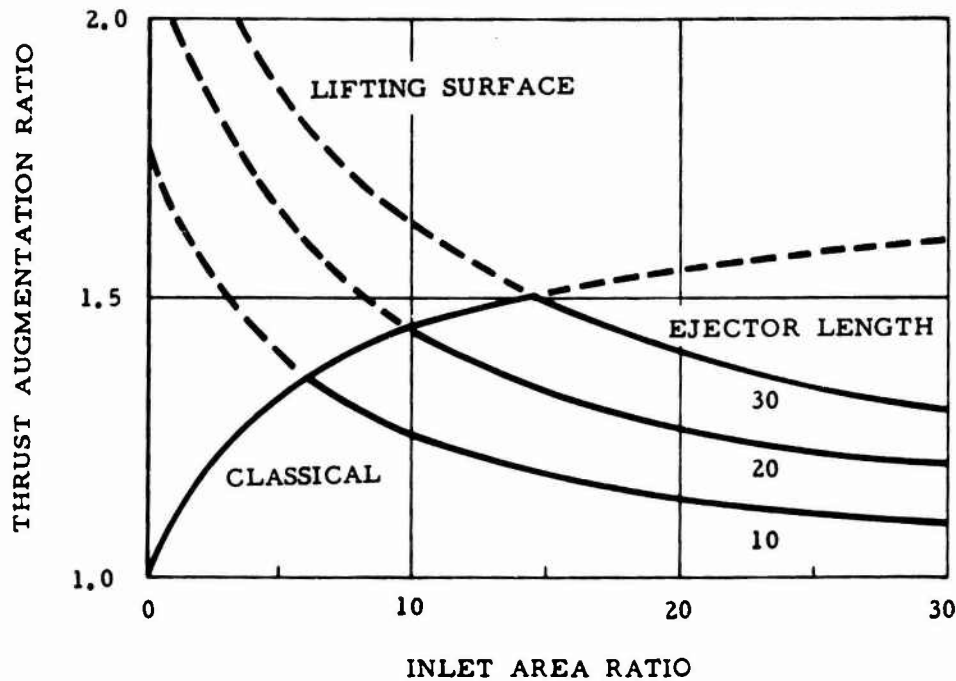


Figure 9. Variation of the Augmentation Ratio for Several Shroud Lengths

varied. It can be seen that in this case, the augmentation ratio actually decreases as the inlet area ratio increases. In the limit as the airfoils are removed to infinity, the augmentation ratio approaches unity, as it must for an isolated turbulent jet. In the opposite limit, as the inlet area ratio approaches unity, an unrealistic increase in the augmentation ratio is obtained. This is because the thickness of the jet has been neglected. The augmentation ratio actually reduces to unity in this limit, as suggested by the classical result also shown in the figure. Since it is based on global conservation of mass and momentum, the classical result puts an upper limit on the augmentation at each inlet area ratio; the intersection with a lifting surface curve is the optimum inlet area ratio for the ejector of given length and specified number of jets and rate of entrainment. The results shown are for a single slot nozzle.

The second important case is that in which the ratio of duct length to throat width L/w is kept constant as the inlet area ratio is varied. This perhaps corresponds more closely to the case implied by the classical methods. The classical result for an ejector without diffusion is a maximum augmentation ratio of $\theta=2.0$ as the inlet area ratio gets infinitely large.¹ The predictions of the present method for this case also are found in Figure 9, by reading across the curves for different duct lengths. No such limit is found; in fact, when the ejector gets very large, the augmentation ratio is not a function of the inlet area ratio at all. It depends only on the length ratio L/w . Of course, for the reasons previously given, the augmentation actually decreases at low inlet area ratios.

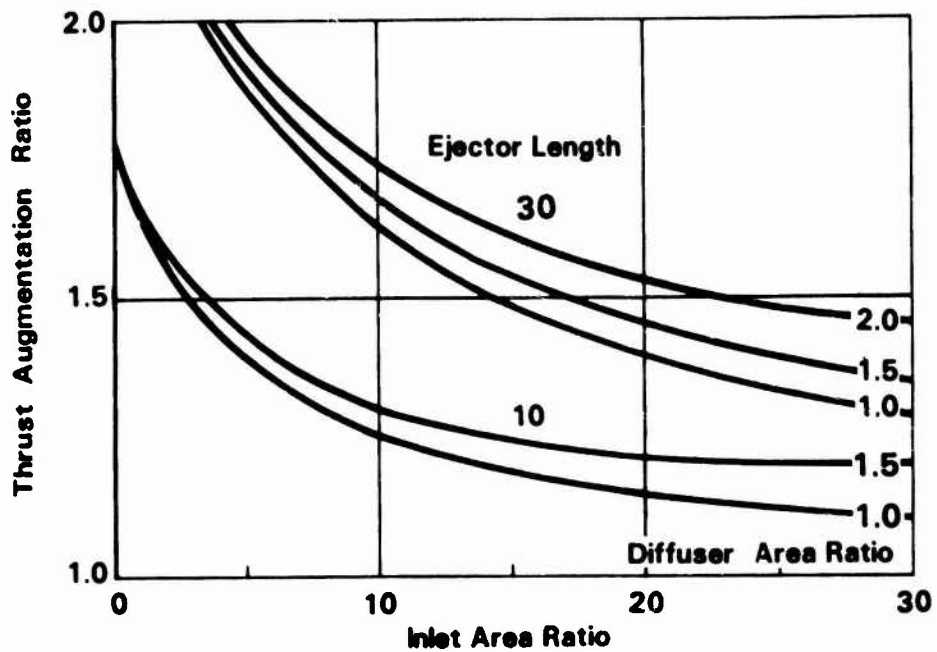


Figure 10. Effect of Diffuser Area Ratio on Thrust Augmentation

The effect of increasing the diffuser area ratio is shown in Figure 10 for two duct lengths. The increase in augmentation with diffuser angle corresponds to the increase in airfoil lift with angle of attack. The augmentation increases with diffuser area ratio over the range shown; but, as the diffusion increases, the airfoils approach 90 deg to the relative wing, and the method breaks down.

The augmentation also depends to some extent on the position of the jet within the shroud. In Figure 11, it can be seen that the optimum location for the nozzle exit

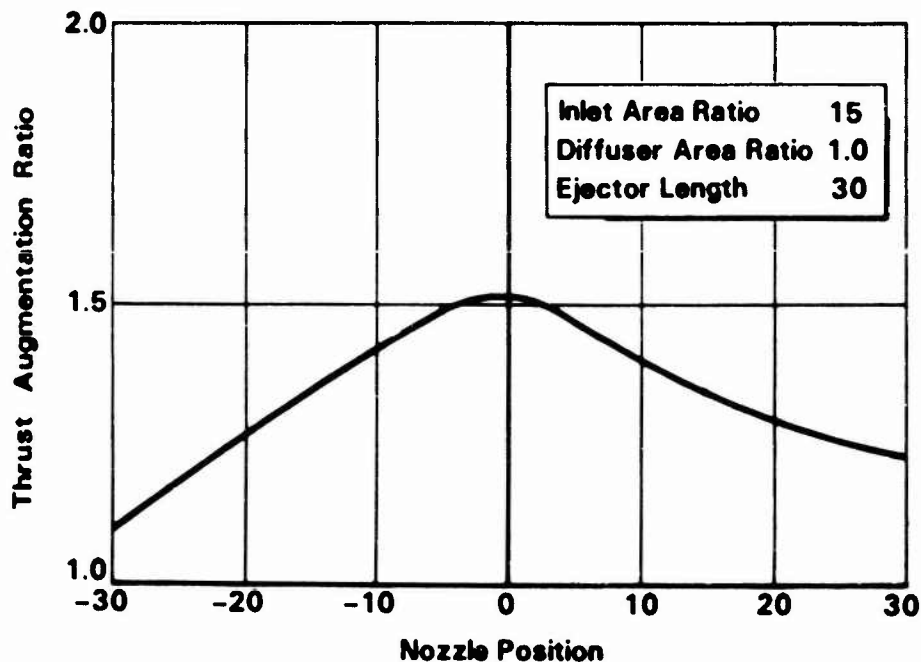


Figure 11. Effect of Nozzle Position on Thrust Augmentation

is in the ejector inlet plane, which is the 0 point in the figure. Actually, if nozzle blockage effects are taken into consideration, the optimum position may be found to be slightly above the inlet plane. The important conclusion is that, within reasonable limits, the nozzle position is not critical.

The effect of changing the rate of jet entrainment can also be estimated with the present method. By arbitrarily varying the value of the entrainment constant defined in Eq. (31), this effect can be calculated. In Figure 12, it is seen that the thrust augmentation increases with $1/R_T$, which is proportional to the von Kármán constant used in simple mixing length theories of jet mixing. The

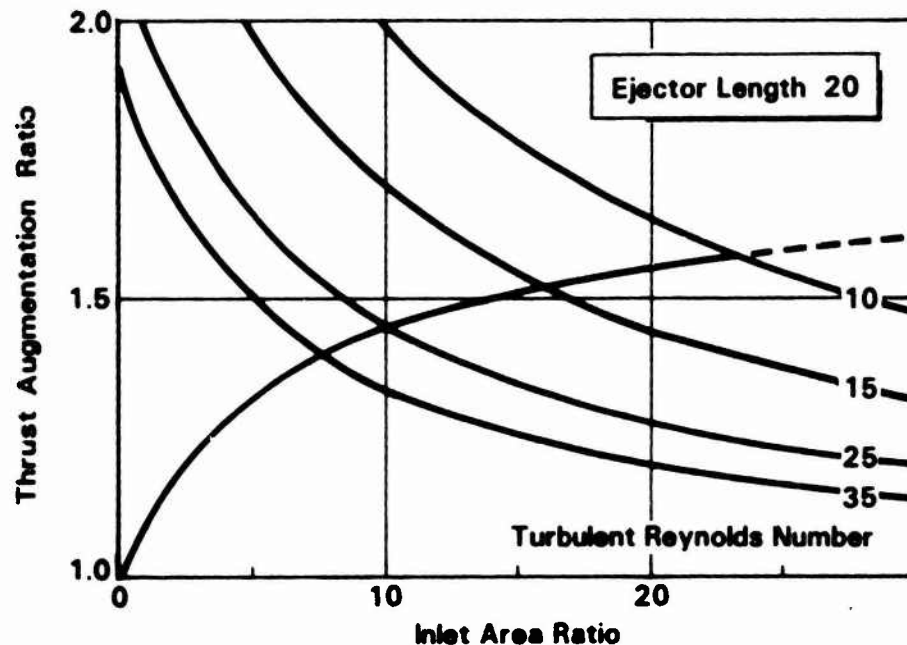


Figure 12. Effect of the Rate of Entrainment on Thrust Augmentation

significance of even small changes in the rate of entrainment is clear. In terms of the force on the shroud, increasing the entrainment corresponds to increasing the speed of the relative wind.

Thus, the present results serve to qualify the conclusions of the classical methods. For constant duct length, the augmentation initially increases with inlet area ratio; but, as the airfoils move out to large distances from the jet, the augmentation reduces to unity. On the other hand, if the duct length is increased with the inlet area ratio, the augmentation remains constant. For either case, the augmentation increases with the diffuser area ratio, up to a limit near where the airfoils become perpendicular to the relative wind. The importance of high rates of entrainment for obtaining high values of augmentation has also been confirmed.

Section Geometry

The hypothesis that the augmenting thrust is related to the lift developed on a wing suggests the use of airfoil high-lift technology to increase the augmentation. Although the ejector thrust corresponds more nearly to a leading-edge suction than to the wing normal force, as seen in Figure 6, both forces depend on the circulation that satisfies the Kutta condition at the trailing edge. Thus, the aerodynamic thrust on the ejector shroud may be expected to depend on the section geometry in the same way as the lift of an airfoil section does. The effect of adding camber and flaperons, or tabs, to the flat-plate ejector shroud will be examined with the lifting surface model in this section.

The change in γ distribution due to camber can be calculated in the planar wing approximation by specifying values of α_i which correspond to the local slope of the camber line for each panel. A simple circular arc section, for which the camber line $z(x)$ is given approximately by

$$z/c = 0.4 \left[(x/c)^2 - (x/c) \right] \quad (32)$$

was investigated. This corresponds to an arc with maximum camber equal to 10% of the chord. The slope of this camber line is

$$\alpha_i = 0.8(x/c) - 0.4 \quad (33)$$

In Figure 13, it can be seen that the effect of camber on the thrust augmentation is very similar to its effect on airfoil lift. The slope of the thrust augmentation curve remains essentially the same, and the thrust at each diffuser area ratio is

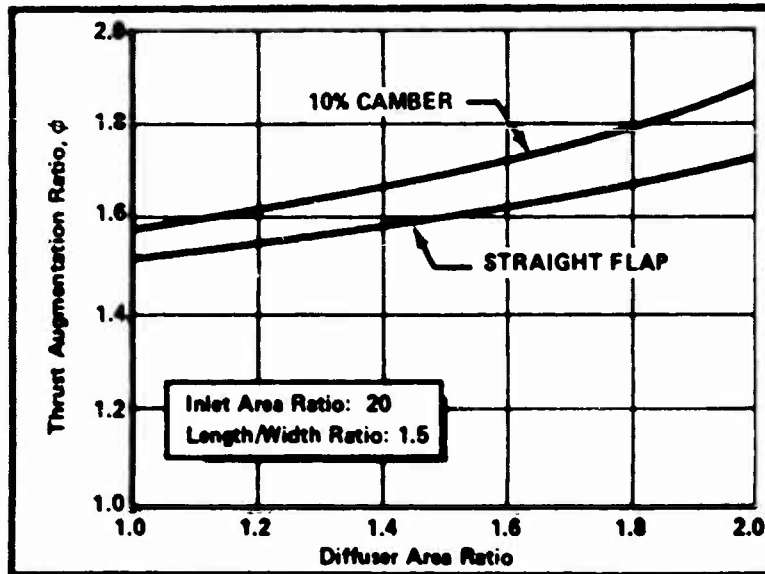


Figure 13. Effect of Camber on Thrust Augmentation

increased by the same amount. As described in the previous section, thrust augmentation is the result of jet mixing in a region of reduced pressure; expressed in these terms, the effect of camber is to further reduce the pressure within the ejector. This produces an increase in the augmentation, as given by Eq. (16).

Deflecting a trailing-edge tab has the effect of changing the camber and angle of attack of the shroud sections. The influence of small deflections can also be calculated with the lifting surface method by specifying appropriate values of α_1 for panels at the trailing edge. In Figure 14, the effect of deflecting 20% of the section chord through an angle of +10 deg is shown. The results again are similar

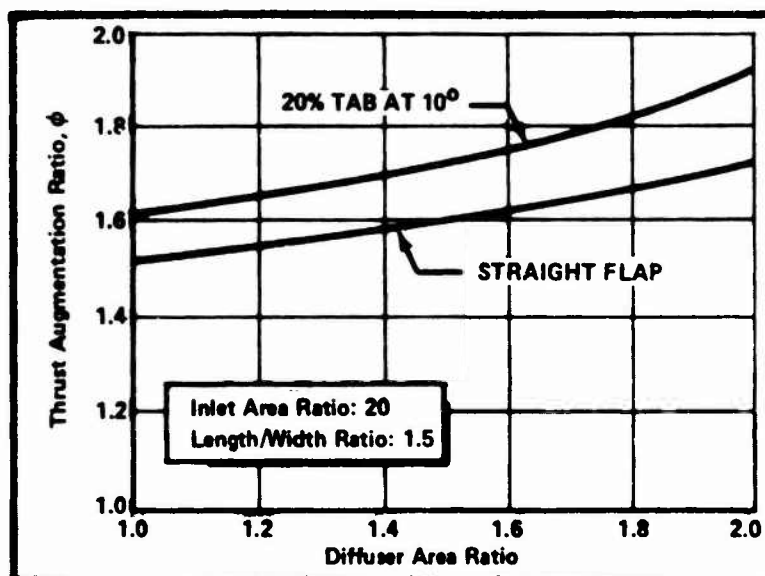


Figure 14. Effect of Trailing Edge Tab on Thrust Augmentation

to airfoil experience. There is a gain in ejector thrust at each angle of attack. However, achieving a gain in ϕ_{\max} depends on keeping the flow attached at large flaperon angles. Since flow separation is a viscous phenomenon, the present inviscid analysis cannot predict the actual increase that may be obtained; but airfoil experience suggests that the stalling angle will be reduced, and the gain in $\Delta\phi$ will be less than predicted.

CONCLUSIONS

The analogy between the lift on an airfoil and the thrust on an ejector shroud provides a more intuitive understanding of the process of ejector thrust augmentation. Thus, the thrust augmentation ratio is seen as analogous to the lift/drag ratio of an airfoil, and the increase in augmentation with the shroud length and diffuser angle is understood in terms of increases in airfoil chord and angle of attack.

In addition, quantitative predictions of the thrust augmentation have been obtained from the airfoil analogy, through the use of vortex panel methods to calculate the forces induced on the ejector shroud. Because elliptic effects are included in the solution, this method of analysis has important advantages over classical methods of calculating the augmentation from the stream thrust. In particular, the effect of varying the length and position of the ejector shroud has been studied. If the ratio of shroud length to throat width is held constant as the inlet area ratio is increased, the augmentation increases slowly, but, if the shroud length is held constant as the inlet area ratio increases, the augmentation actually decreases. These results are in contrast to the classical result, which is that the augmentation increases monotonically with the inlet area ratio.

The analogy also suggests the use of airfoil high-lift technology to increase the thrust augmentation. The effect of adding camber and flaperons to the shroud was calculated with the panel method. The ejector thrust varied in the same way as airfoil lift: over the linear portion of the thrust curve, the augmentation increased the same amount at each diffuser area ratio.

At low inlet area ratios, the analytic method breaks down, because the effect of changes in the rate of entrainment and thickness of the jet is neglected. Work in progress is directed toward improving the method by coupling a parabolic solution for the flow through the ejector to an elliptic solution for the flow outside the ejector. Additional improvements will be obtained by relaxing the planar wing approximation and including the effects of jet thickness.

ACKNOWLEDGEMENT

I would like to acknowledge the contributions of J. R. Williams and J. K. McCullough, who listened to some of my first thoughts regarding this analogy and helped me to develop them.

REFERENCES

- ¹von Kármán, T., "Theoretical Remarks on Thrust Augmentation," Contributions to Applied Mechanics, Reissner Anniversary Volume, J. W. Edwards, Ann Arbor, Mich., 1949, pp. 461-468.
- ²Gilbert, G. E. and Hill, P. G., "Analysis and Testing of Two-Dimensional Slot Nozzle Ejectors with Variable Area Mixing Sections," NASA CR-3351, 1973.
- ³Bevilaqua, P. M., "Evaluation of Hypermixing for Thrust Augmenting Ejectors," Journal of Aircraft, Vol. 11, June 1974, pp. 348-354.
- ⁴DeJode, A. D. and Patankar, S. V., "Prediction of Three-Dimensional Turbulent Mixing in an Ejector," AIAA Journal, Vol. 16, Feb. 1978, pp. 145-150.
- ⁵Viets, H., "Thrust Augmenting Ejector Analogy," Journal of Aircraft, Vol. 14, April 1977, pp. 409-411.

⁶Hancock, G. J., "Comment on Spanwise Distribution of Induced Drag in Subsonic Flow by the Vortex Lattice Method," Journal of Aircraft, Vol. 8, Aug. 1971, p.681.

⁷Kalman, T. P., Giesing, J. P., and Rodden, W. P., "Reply by Authors to G. J. Hancock," Journal of Aircraft, Vol. 8, Aug. 1971, pp. 681-682.

⁸Townsend, A. A., Structure of Turbulent Shear Flow, Cambridge University Press, Cambridge, England, 1976.

⁹McCormick, B. W., Aerodynamics of V/STOL Flight, Academic Press, New York, 1967.

